Coordination Geometries of Zn(II) and Cd(II) in Phosphotriesterase: Influence of Water Molecules in the Active Site

Morris Krauss*

Center Advanced Research Biotechnology/NIST, Rockville, Maryland 20850

Lars Olsen,[†] Jens Antony,[‡] and Lars Hemmingsen[†]

Department of Mathematics and Physics, The Royal Veterinary and Agricultural University, Thorvaldsensvej 40, DK-1871 Frederiksberg C, Denmark, and Bio-Computing Group, Department of Mathematics and Computer Science, Free University of Berlin, Arnimallee 2-6, D-14195 Berlin, Germany

Received: April 1, 2002; In Final Form: June 19, 2002

Models of the metal ion binding sites of native ZnZn and of cadmium-substituted ZnCd and CdCd phosphotriesterase, including full amino acid side chains, were geometry optimized with quantum mechanical methods, with effective fragment potentials (EFP) representing the protein environment surrounding the active site. One to three water molecules were included in the active site in addition to the bridging hydroxide. Comparison with recent X-ray diffraction results {Benning, M. M.; Shim, H.; Raushel, F. M.; Holden, H. M. *Biochemistry* **2001**, *40*, 2712−22} is hindered by the presence of ethylene glycol molecules in the active site. We suggest that the ethylene glycol required for crystallization distorts the structure of the water network in the active site and that the theoretical structures provide a better description of the system in aqueous solution. ^{113}Cd NMR isotropic shielding calculations were performed to analyze the experimentally determined chemical shifts at 212 and 116 ppm, respectively, for the CdCd enzyme. The calculated isotropic shieldings correlate with the coordination number of the metal ions, indicating that the CdCd enzyme has one more ligand at the high shift site than at the low shift site. Theoretically, a number of energetically close structures are found for the CdCd structure. Formally, one of these agrees with the X-ray structure and is supported by the NMR assignment. For the hybrid ZnCd enzyme, the most stable theoretical structure is Cd1Zn2, with the metal bound to the Od1 of the carboxylate of the first-shell aspartate designated M1, but the energy difference between Cd1Zn2 and the lowest energy Zn1Cd2 structure is only about 2 kcal/mol and decreasing with the addition of water molecules. The Zn1Cd2 arrangement is found experimentally.

1. Introduction

Quantum mechanical methods have developed over the past three decades to a stage where they provide an important complementary tool to experimental studies of, among other systems, metal ion containing proteins. For example, such methods allow for detailed studies of electronic properties, reaction pathways, mutations, and metal substitution.[1,2] This study will focus on the organophosphorus hydrolase from *Pseudomonas diminuta*, phosphotriesterase (PTE), which catalyzes the hydrolysis of paraoxon, sarin, soman, and other inhibitors of acetylcholinesterase.[3] X-ray structure determinations for the bimetallic ZnZn[4] and CdCd[5] enzymes initially provided the basis for studying the active site structure and mechanism. Phosphotriesterase has two metal ions bound with two bridging ligands, a hydroxide ion and a carbamylated lysine. Theoretical calculations on the structure of the active site show that the bridging ligand must be anionic hydroxide or the distance between the zinc cations is much larger than observed experimentally.[6−8] As seen in the Figure 1, M1 is also bound to two histidines and an aspartate whereas M2 is bound only to two histidine residues. The Asp301 hydrogen bonded to the bridging hydroxide is a structural motif found often in bimetallic enzymes.[9] The residues toward the protein (the interior) are involved in hydrogen bonds with the first shell of residues. Hydrogen bonds to Od2(Asp301) and Nϵ(His201) could be important in maintaining the conformation and the charge state in the first-shell of the active site. The residues toward solution (the exterior) are predominantly hydrophobic and one residue, Trp131, is quite close to Zn2 and its associated histidines. The role of the hydrophobic residues on the solvent side of the active site is shown by the experimental structure to restrict the orientation of the substrate as well as access of water. The phosphonate inhibitor found in the 1psc structure[5] probably displaces water molecules in the active site. Hydrogen bonding to the Trp131 residue is estimated to be as significant in hydrogen bonding to the water molecules as it is for the inhibitor. The protein environment for the enzymes with different metal ions is found experimentally to be very similar with the backbone atoms superimposed within 0.2 Å in the X-ray structures for the ZnZn and CdCd enzymes.[4,10] Even in vacuo optimized structures have been compared favorably for the low-resolution structure of the enzyme.[11] The in vacuo theoretical structure for the ZnZn enzyme differs mostly from the crystal structure in the orientation of the histidines, His55, His201, and His230, which interact with the bound inhibitor or are hydrogen bonded to an interior residue. The effect of the protein environment on the active site was explored theoretically

* Corresponding author. Tel: 3017386242. E-mail krauss@carb.nist.gov.
[†] The Royal Veterinary and Agricultural University.
[‡] Free University of Berlin.

10.1021/jp025870c CCC: $22.00
Published on Web 08/15/2002

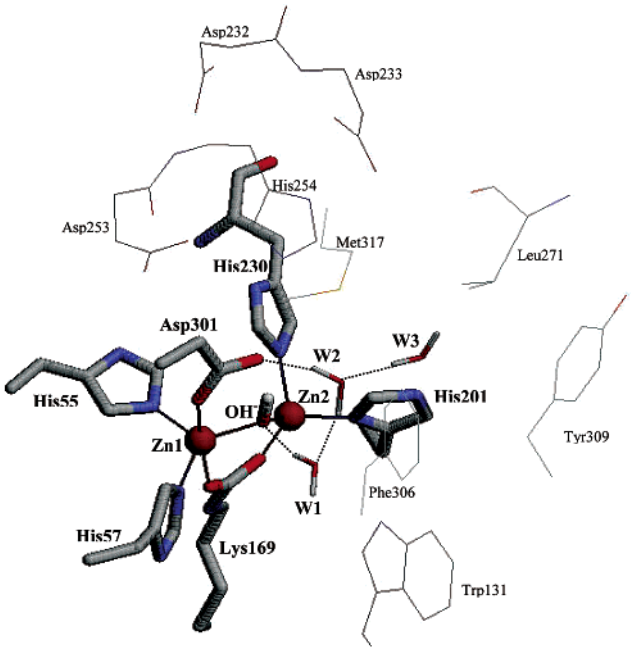

Figure 1. The active site is divided into the quantum region consisting of the models of residues His55, His57, Lys169, His201, His230, Asp301, Zn1, and Zn2, the bridging OH^-, and three water molecules. The local protein environment is represented by the residues Trp131, Asp232, Asp233, Asp253, His254, Leu271, Phe306, Tyr309, and Met317. Interactions between the environment residues and the quantum region are given by the effective fragment potential, EFP. The quantum region is optimized without constraints within the EFP environment.

for the zinc and cadmium enzymes of phosphotriesterase without water ligands for two different charge states.[7] In one, the bridging ligand was a hydroxide anion and in the second the site was protonated at the bridging hydroxide or one of the other ligands. This preliminary analysis of the active site structure found the metal−metal bond distances for ZnZn and CdCd were in good agreement with the X-ray values from the earlier[4,5] relatively low-resolution structures. In addition, the geometry optimized structures are in good agreement with the experimental coordination geometries, i.e., within 0.1 Å (metal ion−ligand bond lengths) and 4° (ligand−metal ion−ligand angles). More recently, higher resolution structures (1.3 Å) have been obtained that apparently provide a detailed picture of the water structure in the active site as a function of metal substitution from the native zinc.[4,10] However, in all of the reported structures including the native zinc enzyme, at least two ethylene glycol molecules are found in the active site. The presence of ethylene glycol molecules required for crystallization in the active site raises the question whether this represents the real structure in solution. The water molecules found in the high-resolution structures, 1hzy (ZnZn), 1i0d (ZnCd), and 1jgm (CdCd),[10] in the protein data bank[12] coexist in the active site with ethylene glycol molecules that are necessary for the crystallization.

The size of the active site requires a methodology that realistically partitions the system into a region treated quantum mechanically (QM region) and an interactive environment. This is possible using the effective fragment potential (EFP) method[13−15] to decompose the quantum Hamiltonian into a quantum fragment interacting with a classical fragment describing the local environment of the active site. The EFP methodology has been applied recently to other enzymes exploring both structural behavior with substrate binding and reactive behavior.[16−18] The phosphotriesterase active site involves hydrogen bonds connecting second and third shell residues to the metal binding complex. These residues are represented by the EFP because their inclusion in the QM region would lead to an intractable calculation.

Because the theoretical structures differ from the crystal structure in various ways, the optimized complexes were used to analyze the solution NMR chemical shifts for ^{113}Cd. For the CdCd enzyme two Cd resonances are observed experimentally at 212 and 116 ppm downfield from $Cd(ClO_4)_2$, whereas for the ZnCd enzyme only a single resonance is observed at 115 ppm.[19] The isotropic shieldings are calculated for the variety of optimized structures with different hydrogen bond arrangements in the active site and compared to the experimental values.

In a recent paper on metallo-β-lactamase,[32] we argue that the water in the active site will have a substantial effect on the electronic properties of the bridging hydroxide and thus the structure and reactivity. A general hydrolysis mechanism for bimetallic hydrolases, e.g., zinc β-lactamase or phosphotriesterase, most likely involves water molecules in the active site, and the uncertainty regarding the water structure implies uncertainty on the mechanism. Redesigning the active site of phosphotriesterase to increase the catalytic effect of the enzyme for a wider variety of nerve gases would require an improved understanding of the mechanism.[4] Because there are two bridging ligands in phosphotriesterase, the interactions between the water molecules and the bridging hydroxide should have a reduced but still significant effect over what has been calculated for the zinc β-lactamase.[32] This study extends the β-lactamase analysis to probe the effect of water binding in the bimetallic active site of phosphotriesterase. The effect of one to three water molecules will be examined and it will be shown that different numbers of water molecules yield substantially different results for the ZnCd enzyme. Although we believe that the smaller number of water molecules is not sufficient to completely represent the solution structure, these structures provide insight into the binding interactions at the first-shell and also may be relevant to nonequilibrium conformations or a prereactive conformation.

2. Methods

With the use of the EFP, ab initio quantum chemical calculations are tractable for an active site that consists of many hundreds of atoms. In this study the protein environment will be restricted to the same used in the earlier study of metal substitution that did not consider the water binding.[7] The EFP integrals and gradients have been implemented in GAMESS.[20] The current implementation of the EFP method includes Coulombic, polarization (classical induction), and nonbonded exchange repulsion.[16−18] In the present implementation, the Coulombic and polarization terms are calculated directly within GAMESS.[20] The repulsive terms are obtained by fitting the interactions of the all-electron terms for the expected orientations with the hydrogen-bonded interactions for the hydrophilic residues and the overlap repulsions for the hydrophobic ones. The repulsive EFP were parametrized with the assumption that a water molecule probe can simulate the range of interactions.

The first-shell active site, treated quantum mechanically, is defined as described in Figure 1 to consist of the two metal cations and the following ligands: Asp301, His55, His57, His230, His201, Lys169 with the lysine carbamylated. For these residues all atoms are included back to the C_α atom. In one case, H230, the amide backbone was also included because there are backbone hydrogen-bonded interactions to the interior protein. All the imidazole ligands (histidines) are maintained neutral. The protein environment is represented by EFP with

all the neighboring residues fixed at the positions found in the low-resolution ZnZn enzyme for all calculations.[4] The residues represented by EFP are Trp131, Asp232, Asp233, His254, Asp253, Leu271, Met317, Phe306, and Tyr309. His254 is in a hydrogen bond environment that dictates this residue to be protonated.

All geometry optimizations were carried out at the Hartree−Fock level using the CEP 4-31G basis set concomitant to the effective core potentials.[21,22] The Zn−Zn active site was optimized with the C_α atoms unconstrained and three water molecules present. This is to provide a theoretical structure to compare both the other theoretical structures as well as the recent high-resolution crystal structures (1hzy). For the ZnCd and Cd−Cd active sites the C_α are constrained at the crystal coordinates or unconstrained in the optimization allowing the EFP interactions to restrain the motions of the QM fragment residues. The default condition for optimization in GAMESS was not always achieved because the number of iterations would then exceed 300 and required a large amount of computer time. Nevertheless, all runs were converged to a maximum RMSD below 0.0005 au. The large number of degrees of freedom is an essential difficulty compounded by the strong coupling between high and low frequency modes leading to a rather soft effective potential around the metal cations. The X-ray structure finds two water molecules bound to Cd2 in both the ZnCd and CdCd structure and we initiated optimizations with these structures but found that the two water molecules remain bound to Cd2 only for the CdCd case. Three ZnCd and four CdCd water binding arrangements will be presented and discussed below.

NMR isotropic shieldings were calculated for truncated versions of the optimized structures. The structures were truncated by breaking bonds and saturate with hydrogen atoms pointing in the same direction as the broken bond. Imidazole rings were used for the histidines, CH_3COO^- for the aspartic acid, and CH_3NHCOO^- for the carbamylated lysine. The C−H bond lengths for the saturating hydrogen atoms were chosen as 1.08 Å in imidazole rings, and 1.10 Å in methyl groups. These distances are in accordance with the C−H bond lengths in the imidazole rings and CH_3 groups of the optimized structures. Three water molecules were included in the calculations in addition to the bridging hydroxide. The resulting model system consisted of $M1M2(Im)_4(CH_3COO)(CH_3NHCOO)(OH)(H_2O)_n](H_2O)_{3-n}^+$, where Im is a short notation for imidazole rings and M1 and M2 for the metal ions in site 1 and site 2. The effect of having imidazoles as models of histidines was investigated by calculating the NMR isotropic shieldings for one case with the imidazole replaced by methylimidazole, giving differences of less than 3 ppm. The B3LYP density functional method[23−25] was applied with the uncontracted form of the basis set of Kellö and Sadlej[26] on cadmium and 6-31G(d)[27] on the ligand atoms and zinc. The NMR shielding tensors were computed with the gauge-independent atomic orbital (GIAO) method.[28] Using this method and basis sets gives an average error of about 50 ppm for differences of isotropic shieldings between different cadmium-containing model systems[29] and the experimental result. The calculations were performed with the Gaussian98 program[30] on PCs with a Linux operating system.

3. Results and Discussion

3.1. Active Site with Three Water Molecules. *Zn1Zn2 Structures.* The ZnZn theoretical structure (Figure 1) predicts one pentacoordinate site at Zn1 and a tetracoordinate site at Zn2. The initial structure in the optimization had W3 bound to Zn1 and W2 to Zn2 but both dissociated in the course of the optimization. In the optimized structure, the water, W1, is directly hydrogen-bonded to the bridging hydroxide and W3 is hydrogen-bonded to both W1 and the Od2 of the aspartate carboxylate. In the starting conformation W2 has a weak interaction to W1 but this gets stronger during the optimization and the bond between Zn2 and W2 is broken, leading ultimately to the hydrogen-bond network of W2−(2.71 Å)−W3−(2.84 Å)−Od2(asp) and W1−(2.73 Å)−W3. The effective charge on Zn2 is sufficiently less than 2, and the water−water hydrogen bonds are stronger in this model. The hydrogen bond from Trp131 to W2 seen in the crystal structure is constructed for the initial structure in the optimization but converts to a weak hydrogen bond to W1. The structure is shown with the EFP environment in Figure 1 for the ZnZn case. This environment is the same for all structures and, for clarity, will not be included in the remaining figures.

The optimized theoretical structure is not observed in the crystal structure, 1hzy. In active site A, there is one Zn2−W2 bond with a bond length of 2.1 Å. W2 is within hydrogen-bonding distance of the tryptophan and ethylene glycol. An ethylene glycol molecule is close enough to prevent any other water molecules binding to the first shell. In active site B, the Zn2−W2 bond length is 2.4 Å with W2 in hydrogen bond proximity of tryptophan and ethylene glycol. The predicted ZnZn distance of 3.45 Å is about the same as the experimental value but it is sensitive to W1 hydrogen bonding to the bridging hydroxide. Proton donation from W1 to the hydroxide tends to increase the metal−metal distance probably due to a reduction of the effective charge of the bridging hydroxide. The binding of W2 to W1 tends to increase the hydrogen bonding distance from W1 to the hydroxide during the course of the optimization. This decreases the effective proton donation to the hydroxide and the calculated ZnZn distance agrees more closely with experiment. Protonation of the bridging hydroxide has been shown to lead to large metal metal distances in phosphotriesterase[6,7] and in zinc β-lactamase.[31,32] The partial donation of a proton has a proportionate effect.

The apparent contradiction between the experimental and theoretical hydrogen bonding network is most likely related to the presence of ethylene glycol molecules in the crystal. Both active sites A and B of the ZnZn structure have an ethylene glycol molecule hydrogen-bonded to both the bridging hydroxide at a distance of 3.2 Å and to W2 at a distance of 2.6 Å. In active site B, W2 is also weakly hydrogen bonded to two other water molecules at distances of 3.0 and 3.2 Å. There are also two ethylene glycol molecules hydrogen bonded to the hydroxide in active site B, accounting, perhaps, for the displacement of water from this binding arrangement. The lack of similarity between active sites A and B suggests that a number of local minima are accessible for water binding in the active site. The theoretical calculation suggests that networks of hydrogen-bonded water molecules occur and that the water bound to the hydroxide constitutes a central position. With this water molecule displaced by one or more ethylene glycol molecules, the entire network is disturbed. Developing the network of water molecules toward solution could tend to stabilize the water bound to Zn2, as indicated in active site B. In summary, removing the ethylene glycol molecules and including a number of water molecules results in a change of the coordination geometry at both metal ion binding sites. The coordination number is decreased by 1 at both sites, because two water molecules leave the first shell to participate in the local hydrogen bonding network. We consider the model systems presented here to be more realistic models of the metal ion binding sites in

solution, because the ethylene glycol molecules, obviously, cannot be present.

Zn1Cd2 and Cd1Zn2 Structures. In addition to the arrangement of water molecules bound to the first shell, it is of interest to determine the relative energies of the Zn1Cd2 and Cd1Zn2 enzymes. The crystal structure has a Zn1Cd2 arrangement of the metal ions, with two water molecules bound to Cd2. The experimental schematic shows two water molecules at a distance of 2.8 and 2.5 Å from Zn2 although the distances in pdb structure 1jgm in the two independent sites differ from the schematic by up to 0.2 Å. Weak interactions from the water molecules are possible to Trp131, His254, between the water molecules, and to the bridging hydroxide but, again, water strongly interacting with the bridging hydroxide or other ligands would be hindered by the ethylene glycols. Oxygen from the ethylene glycols is within 2.9 Å of the bridging hydroxide. None of the theoretical structures have two water molecules bound to Cd2 (see Figures 2a−c), even though this was one initial structure in the optimizations.

The lowest energy theoretical CdZn structure has a water molecule bound to Cd1 (Figure 2a). The next two lowest energy theoretical structures are one with Cd1Zn2 (Figure 2b), which is higher in energy by about 1.5 kcal/mol, and one with Zn1Cd2, which is additionally less than 1 kcal/mol higher in energy (Figure 2c). These structures are so close in energy that they are considered essentially equivalent at the level of accuracy of the calculations presented here. The lowest energy optimized structure (Figure 2a) is hexacoordinate at Cd1 with a Cd1−W3 distance of 2.46 Å. W3 is hydrogen bonded to W1 (2.76 Å), which hydrogen bonds to the bridging hydroxide. W2 makes a hydrogen bond to W1 (2.83 Å) and also to the Od2 of the Asp301. With two water molecules hydrogen bonding to W1, the hydroxide is only slightly screened by partial proton donation and the CdZn distance lengthens slightly to 3.70 Å, that is, only 0.1 Å larger than the experimental value. Constraining the C_α atoms of the residues and reoptimizing 2a leads to relatively small changes and an energy increase of only 3 kcal/mol, suggesting the EFP residues constrain the first shell realistically. The next lowest energy structure (Figure 2b) has no water molecules bound to Cd1 or Zn2. Although W1 was initially bound to Cd1 and W2 to Zn2, both W2 and W1 moved far from either metal ion during the optimization, with W2 hydrogen bonded to W1 (2.69 Å), which in turn donates a proton to the bridging hydroxide with a short hydrogen bond, O(W1)−O(bridge) (2.65 Å). W3 hydrogen bonds to Od1 of the carbamylated lysine. The theoretical structure, 2c, started with two water molecules bound to Cd2, and the optimization ends with a Cd2−W2 bond length of 2.52 Å. This water molecule is hydrogen bonded to W3 (2.62 Å), which in turn hydrogen bonds to Od2 of the aspartate carboxylate as well as W1 (2.76 Å), which hydrogen bonds to the bridging hydroxide. In this case the Zn1Cd2 distance has a relatively large value of 3.80 Å.

The experimental structure of the hybrid, 1jgm, shows bond lengths of 2.4 and 2.8 Å for W2 and W1 bound to Cd2. W2 has possible hydrogen bonds to another water molecule, 2.9 Å, to the bridging hydroxide, 2.8 Å, and to an ethylene glycol, etg1, with a distance of 3.2 Å. W1 is within 2.9 Å of the bridging hydroxide. Another ethylene glycol, etg2, effectively hydrogen bonds to the hydroxide at 2.9 Å. There are three connected hydrogen bonds that stabilize W1 and W2 to a common water molecule and connect W2 to etg1. In summary, the second shell of water and ethylene glycol in the experimentally determined structure apparently stabilizes the water molecule(s) bound to

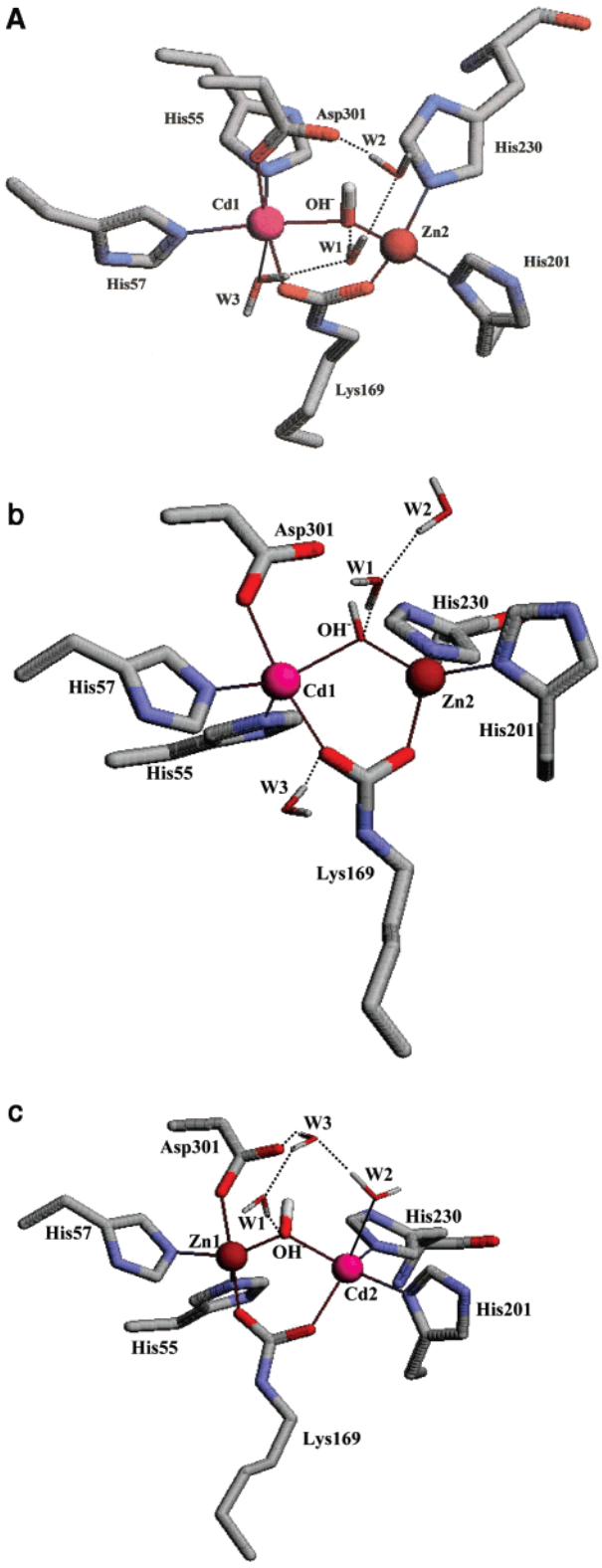

Figure 2. Unconstrained optimized models for ZnCd structures with three water molecules (the protein environment is identical to that used for the native ZnZn active site in Figure 1). (a) Cd1Zn2 with W3 coordinating to Cd1 and water network W3−W1−W2. W1 is always hydrogen bonded to OH. (b) Cd1Zn2 with no water molecules bound to the metal ions and W2 hydrogen bonded to W1 with W3 is hydrogen bonded to the carbamylated lysine. (c) Zn1Cd2 with W2 coordinating to Cd2 and water network W2−W3−W1.

Cd2 and one or two ethylene glycol molecules always interacts with the hydroxide. This artificially causes higher coordination numbers than those found in this work. It is, however, possible

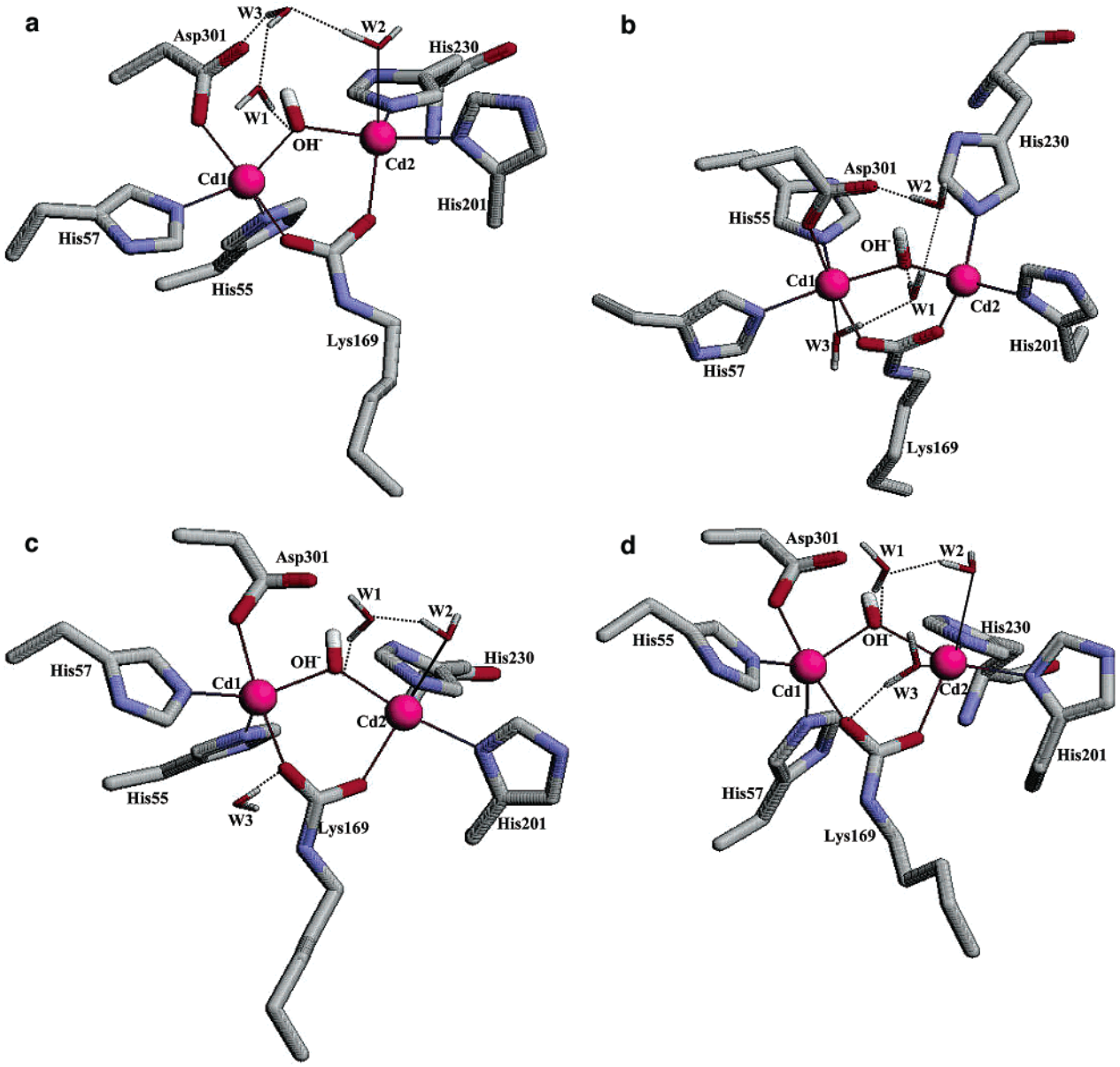

Figure 3. Unconstrained optimized models for CdCd structures with three waters (the protein environment is identical to that used for the native ZnZn active site in Figure 1). (a) W2 coordinating to Cd2 and water network W2—W3—W1. W1 is always bound to OH. (b) W3 coordinating to Cd1 and network W3—W1—W2. (c) W2 coordinating to Cd2, W2 hydrogen bonded to W1, and W3 hydrogen bonded to the carbamylated lysine. (d) W2 and W3 coordinating to Cd2, W2 hydrogen bonded to W1, and W3 hydrogen bonding to the carbamylated lysine.

that inclusion of more than three water molecules could also stabilize the coordination of water molecules to the metal ions.

Cd1Cd2 Structures. For the CdCd structures, local minima are found for a number of different arrangements of the hydrogen-bonded water network in the active site. Even though both constrained and unconstrained optimizations were used, the relative energies of the complexes are within 2 kcal/mol, that is, very close. The structures are shown in Figure 3 in order of the increasing calculated energy. The lowest energy structure (Figure 3a) shows a hydrogen bonding network connecting the water, W1, bound to the hydroxide, to W3 that binds to the Od2 carboxylate of the aspartate. The water W3 is bound to W2 (2.67 Å) which coordinates to Cd2 (2.53 Å). W2 is substantially polarized as seen in the OH bond donating to W3 having a bond length of 1.00 Å. In the next structure (Figure 3b), the water, W3, bound to Cd1 (2.47 Å) is part of a network that connects to W1 (2.74 Å), which binds to the hydroxide (2.64 Å), and to W2 (2.86 Å) that is bound to the Od2 of the aspartate carboxylate. In the third structure W2 (Figure 3c) is bound to Cd2 (2.59 Å) and hydrogen bonded to W1 (2.60 Å) that in turn binds to the hydroxide (2.61 Å). W3 stands alone and hydrogen bonds to the Od1 of the carbamylated lysine. The only optimized structure with two water molecules (Figure 3d) bound to Cd2 (W2 2.43, W3 2.67 Å) also shows that these water molecules hydrogen bond to either another water, W1, or to the carbamylated lysine. The central position of W1 that hydrogen bonds to the hydroxide is found in all the structures. The calculated energy separating these structures is relatively small when the method applied and the restrictions on the environment are considered. No attempt was made to find all such water networks because of the computational expense.

In the high-resolution experimental structure (1jgm), surprisingly, the two crystallographically independent sites (each comprising a binuclear site) are substantially different in the terms of water positions and also differ from the schematic of the experimental active site.[10] For example, in active site B two water molecules both have bond lengths to the cadmium of about 2.5 Å whereas the schematic has one water at 2.5 Å and the

TABLE 1: Calculated NMR ^{113}Cd Isotropic Shieldings (ppm) for Geometry Optimized Metal Ion Binding Sites of Phosphotriesterase

	site 1		site 2	
	coord no.	isotropic shielding (ppm)	coord no.	isotropic shielding (ppm)
Figure 2a	6	3772	4	
Figure 2b	5	3686	4	
Figure 2c	5		5	3697
Figure 3a	5	3630	5	3683
Figure 3b	6	3763	4	3558
Figure 3c	5	3679	5	3691
Figure 3d	5	3639	6	3754

other at 2.0 Å. The bridging hydroxide is within hydrogen-bonding distance of two ethylene glycol molecules (2.6, 2.8 Å) preventing any water from binding. In active site A of the CdCd structure there is a Cd−W2 bond with a bond length of 1.55 Å that is too short to be correct. A water molecule is also found to bind to the Od2 carboxylate atom of the first-shell aspartate, which will interfere with any water binding to the bridging hydroxide. Interestingly, there is another water molecule in this structure that hydrogen bonds to the hydroxide (2.5 Å) at an angle similar to that found in the theoretical structure for W1 hydrogen bonding to the hydroxide. The only ethylene glycol in this site is bound to W2, relatively far from the hydroxide. In active site B two ethylene glycols are within 2.8 Å of the hydroxide but there is a water molecule near the hydroxide that acts like W1 in the theoretical structure and also binds to Od2 of the aspartate carboxylate and to W3. Both of the above-described water molecules have two hydrogen bonds from either water or ethylene glycol that stabilize the bond to Cd2.

In summary, also for the CdCd enzyme, the presence of the ethylene glycol molecules disrupts the hydrogen-bonding network found in this work at the metal ion binding sites. It is noteworthy that a water molecule, corresponding to W1 in this work, appears in the experimental structure, when the ethylene glycol molecules are relatively far away from the hydroxide ion, supporting the contention that this water molecule is present in the real solution structure.

Calculated ^{113}Cd NMR Isotropic Shieldings. The calculated isotropic shieldings, Table 1, indicate that the most important factor controlling the shielding, in the case of phosphotriesterase, is the coordination number of the metal ions. Independent of which of the two sites is occupied with cadmium, a six-coordinated site has the highest shielding (lowest chemical shift) of 3754−3772 ppm. A five-coordinated site has a shielding that is about 100 ppm lower, and the only four-coordinated site is additionally about 100 ppm less shielded. The experimentally determined shifts are 212 and 116 ppm (relative to $Cd(ClO_4)_2$) for the CdCd enzyme. The difference of about 100 ppm indicates that the higher shift corresponds to a site with a coordination number of one lower than the low shift site. In the experimental ^{113}Cd NMR spectra two signals are observed. The most straightforward interpretation is that these originate from each of the two sites, indicating that only one of the energetically close optimized CdCd enzyme structures is observed in solution. Alternatively, rapid exchange between a number of water network structures could also result in two well-defined peaks in the spectra. In phosphotriesterase, site 1 has five metal ion coordinating atoms from the protein and site 2 has four atoms metal ion coordinating from the protein. In addition, there are a number of possibly coordinating water molecules. This gives three possible coordination geometries that can agree with the interpretation of a difference in coordination number of 1 between the two sites: coordination numbers of 5:4, 6:5, or 5:6 for site1:site2. The 5:4 coordination number is in contradiction with all X-ray diffraction data, and it seems unlikely that no water molecules should coordinate to cadmium in a water accessible active site. However, as described above, it is possible that the presence of the ethylene glycol molecules in the crystals artificially stabilizes the binding of water molecules to the metal ions. Therefore, this possibility (5:4) cannot be ruled out. The 5:6 arrangement is consistent with the crystal structure and, furthermore, is found in one of the geometry optimized structures, 3d. Finally, the 6:5 arrangement is also possible, though none of the geometry optimizations converged to this structure, and it does not agree with the experimentally determined structures. The other predicted structures, Figures 3a−c, do not satisfy the NMR shift observed in solution. In the ZnCd hybrid enzyme the measured shift is 115 ppm, probably corresponding to the lower shift in the CdCd enzyme. This indicates that the cadmium ion in the hybrid enzyme occupies the same site as the one that has the highest coordination number in the CdCd enzyme. Structure 2a is consistent with the shift assignment, but this does not agree with the crystal structure that suggests two water molecules bound to Cd2. However, one of the two water molecules does have a large bond distance, and as noted above, the active site binds ethylene glycol, which interferes with the water structure.

3.2. Active Site in the ZnCd Hybrid Enzyme with Less Than Three Water Molecules. In a preliminary paper[7] in this series of observations on the phosphotriesterase active site, the ZnZn and CdCd enzymes were examined without any water molecules present. The unconstrained optimizations yield a first-shell active site that is qualitatively similar to the present results with water and, as noted above, predict metal−metal bond distances in better agreement with the experimental values. Bidentate aspartate binding is obtained when the C_α atoms are frozen in the optimization of the CdCd enzyme. This is also true for the constrained optimization of Cd1Zn2. Bidentate binding is driven by the short CdZn bond distance of 3.46 Å and the propensity of the Cd coordination sphere to incorporate five or six ligands. For Zn1Cd2 the binding of Zn1 to the aspartate remains monodentate, as expected, and the ZnCd distance is 3.52 Å. The Zn1Cd2 structure is about 9 kcal/mol higher in energy than Cd1Zn2. This difference may be due to the fact that the M1 site has a higher coordination number, which is easier to achieve with the larger cadmium ion. The structures with one or two added water molecules are of interest as possible intermediates in reactive high-energy cases or the possibility that substrate binding can restrict the number of water molecules to less than 3. The substrate presence would also alter the inherent behavior just as the ethylene glycol molecules do in the crystal structure.

With one water molecule, the lowest energy structure (Figure 4a) obtained is unusual at first glance with a long distance of 3.78 Å between Cd1 and Zn2. The active site separates into two complexes bridged by the carbamylated lysine assisted by a hydrogen bond between the water molecule bound to Cd1 (2.38 Å) and the formerly bridging hydroxide that remains bound to Zn2 (1.93 Å). The aspartate carboxylate is bound in bidentate arrangement to Cd1, reflecting the larger coordination number of Cd. This structure is about 7 kcal/mol lower in energy than the lowest energy structure for Zn1Cd2 (Figure 4b), where the water molecule binds to the bridging hydroxide. This phenomenon has been observed in zinc β-lactamase[31,32] and may be a general phenomenon in bimetallic enzymes. Additional water molecules will screen the metal bound water, lowering the propensity to donate the proton. When the water molecule

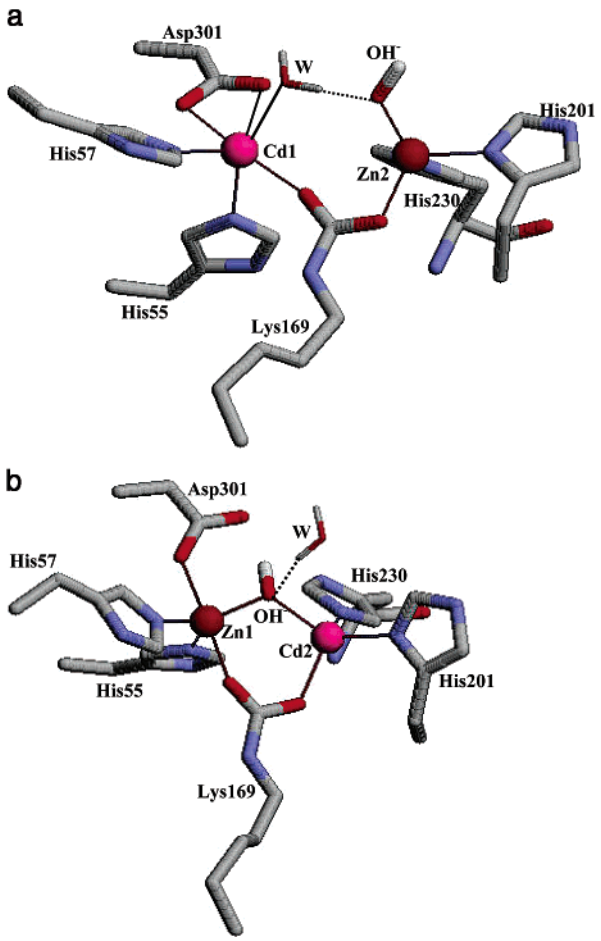

Figure 4. Unconstrained optimized models for ZnCd structures with one water (the protein environment is identical to that used for the native ZnZn active site in Figure 1). (a) Cd1Zn2, The water molecule coordinated to Cd1. OH no longer bridges Cd1 and Zn2 but is bound to Zn2 and hydrogen bonded to the water molecule. (b) Zn1Cd2, with the water molecule hydrogen bonded to bridging OH.

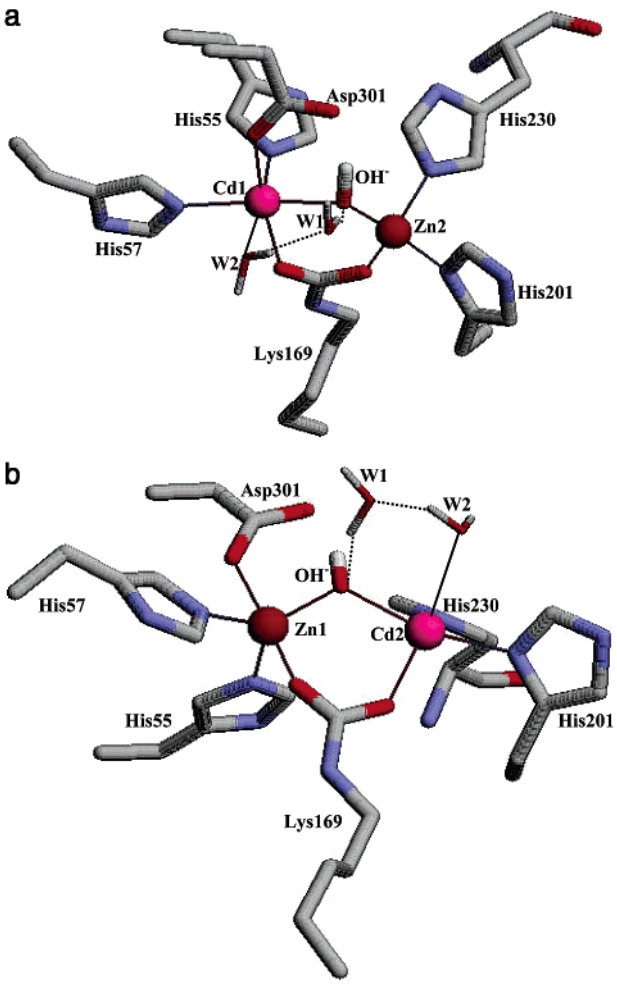

Figure 5. Unconstrained optimized models for ZnCd structures with two water molecules (the protein environment is identical to that used for the native ZnZn active site in Figure 1). (a) Cd1Zn2, with W2 coordinating to Cd1 and W2−W1−OH network. (b) Zn1Cd2, W2 coordinating to Cd2 and W2−W1−OH network.

is bound to Cd2, this metal ion does not activate the water molecule sufficiently so that the interaction with the bridging hydroxide results in hydrogen bonding rather than the separation of the metal cations. This was also observed for the cadmium-substituted zinc β-lactamase.[31,32]

With two water molecules in the active site, the Cd1Zn2 structure (Figure 5a) is lower in energy by 5 kcal/mol than the Zn1Cd2 (Figure 5b). The water molecule bound to Cd1 (2.46 Å) in 5a is hydrogen bonded to W1 (2.83 Å), the water hydrogen bonded to the bridging hydroxide. In 5b the water molecule is bound to Cd2 (2.59 Å) and it also hydrogen bonds to the water (2.60 Å) bound to the bridging hydroxide. The central role of the water bound to the bridging hydroxide is found as soon as there are two waters in the active site. The Cd1Zn2 structure has an octahedral coordination around Cd1 and tetrahedral around Zn2, whereas Zn1Cd2 has two distorted trigonal bipyramids. The low propensity for the Zn to be five-coordinate accounts for the higher energy of the structure with the Cd at site 2. When there are three water molecules present in the active site, the energy difference between the Cd1Zn2 and Zn1Cd2 is reduced to 1.5 kcal/mol, suggesting that the lowest energy position for the Cd replacement is dependent on the hydrogen-bonding network. As noted above, not only is the number of water molecules insufficient to provide a conclusive answer to this question but the present EFP environment is frozen and dynamics could play a significant role.

4. Conclusion

In this work we have presented geometry optimized model systems of the metal ion binding sites of ZnZn, ZnCd, and CdCd phosphotriesterase, with particular focus on the effect of water molecules in the active site and the hydrogen-bonding network. This was done as an effort to make realistic models of the solution structure of the metal ion binding sites, eliminating the problematic ethylene glycol molecules found in the published crystal structures. In addition to the geometry optimizations, we performed calculations of the isotropic shieldings of ^{113}Cd in the complexes, using the experimentally determined chemical shifts (116 and 212 ppm)[19] as fixed points to be reproduced by the calculations. The calculated shieldings indicate that there is a difference in coordination number of 1 between the two sites, and this may be represented by the structure shown in Figure 3d. The geometry optimizations show that the water molecules make a local hydrogen bonding network that is not found in the crystal structures due to the presence of the ethylene glycol molecules. An important role is found for a water molecule, which hydrogen bonds to the bridging hydroxyl and to the anionic ligands in the active site. This is important because the calculations show that the network of waters bound to ionic ligands in the first shell yields polarized and activated waters that may have a function in the enzymatic hydrolysis reaction.

References and Notes

(1) Siegbahn, P. E. M.; Blomberg, M. R. A. *Annu. Rev. Phys. Chem.* **1999**, *50*, 221−49.

(2) Siegbahn, P. E. M.; Blomberg, M. R. A. *Chem. Rev.* **2000**, *100*, 421−37.

(3) Raushel, F. M.; Holden, H. M. *Adv. Enzymol. Relat. Areas Mol. Biol.* **2000**, *74*, 51−93.

(4) Vanhooke, J. L.; Benning, M. M.; Raushel, F. M.; Holden, H. M. *Biochemistry* **1996**, *35*, 6020−5.

(5) Benning, M. M.; Kuo, J. M.; Raushel, F. M.; Holden, H. M. *Biochemistry* **1995**, *34*, 7973−8.

(6) Zhan, C. G.; deSouza, O. N.; Rittenhouse, R.; Ornstein, R. L. *J. Am. Chem. Soc.* **1999**, *121*, 7279−82.

(7) Krauss, M. *J. Chem. Inf. Comput. Sci.* **2001**, *41*, 8−17.

(8) Koca, J.; Zhan, C. G.; Rittenhouse, R. C.; Ornstein, R. L. *J. Am. Chem. Soc.* **2000**, *123*, 817−26.

(9) Wilcox, D. E. *Chem. Rev.* **1996**, *96*, 2435−58.

(10) Benning, M. M.; Shim, H.; Raushel, F. M.; Holden, H. M. *Biochemistry* **2001**, *40*, 2712−22.

(11) Kafafi, S.; Krauss, M. *Int. J. Quantum Chem.* **1999**, *75*, 289−99.

(12) Berman, H. M.; Westbrook, J.; Feng, Z.; Gilliland, G.; Bhat, T. N.; Weissig, H.; Shindyalov, I. N.; Bourne, P. E. *Nucl. Acids Res.* **2000**, *28*, 235−42.

(13) Day, P. N.; Jensen, J. H.; Gordon, M. S.; Webb, S. P.; Stevens, W. J.; Krauss, M.; Garmer, D.; Basch, H.; Cohen, D. *J. Chem. Phys.* **1996**, *105*, 1968−86.

(14) Worthington, S. E.; Krauss, M. *Comput. Chem.* **2000**, *24*, 275−85.

(15) Gordon, M. S.; Freitag, M. A.; Bandyopadhyay, P.; Jensen, J. H.; Kairys, V.; Stevens, W. J. *J. Phys. Chem. A* **2001**, *105*, 293−307.

(16) Richter, U.; Krauss, M. *J. Am. Chem. Soc.* **2001**, *123*, 6973−82.

(17) Worthington, S. E.; Roitberg, A. E.; Krauss, M. *J. Phys. Chem. B* **2001**, *105*, 7087−95.

(18) Worthington, S. E.; Krauss, M. *J. Phys. Chem. B*, in press.

(19) Omburo, G. A.; Mullins, L. S.; Raushel, F. M. *Biochemistry* **1993**, *32*, 9148−55.

(20) Schmidt, M. W.; Baldridge, K. K.; Boatz, J. A.; Elbert, S. T.; Gordon, M. S.; Jensen, J. H.; Koseki, S.; Matsunaga, N.; Nguyen, K. A.; Su, S. J.; Windus, T. L.; Dupuis, M.; Montgomery, J. A. *J. Comput. Chem.* **1993**, *4*, 1347−63.

(21) Stevens, W. J.; Basch, H.; Krauss, M. *J. Chem. Phys.* **1984**, *81*, 6026−33.

(22) Stevens, W. J.; Krauss, M.; Basch, H.; Jasien, P. G. *Can. J. Chem.* **1992**, *70*, 612−30.

(23) Lee, C.; Yang, W.; Parr, R. W. *Phys. Rev.* **1988**, *B37*, 785−9.

(24) Becke, A. D. *J. Chem. Phys.* **1993**, *98*, 1372−7.

(25) Becke, A. D. *J. Chem. Phys.* **1993**, *98*, 5648−52.

(26) Kellö, V.; Sadlej, A. J. *Theor. Chim. Acta* **1995**, *91*, 353−71.

(27) Hehre, W. J.; Ditchfield, R.; Pople, J. A. *J. Chem. Phys.* **1972**, *56*, 2257−61.

(28) Wolinski, K.; Hilton, J. F.; Pulay, P. *J. Am. Chem. Soc.* **1990**, *112*, 8251−60.

(29) Antony, J.; Olsen, L., Hemmingsen, L. Manuscript in preparation.

(30) Frisch, M. J.; Trucks, G. W.; Schlegel, H. B.; Scuseria, G. E.; Robb, M. A.; Cheeseman, J. R.; Zakrzewski, V. G.; Montgomery, J. A., Jr.; Stratmann, R. E.; Burant, J. C.; Dapprich, S.; Millam, J. M.; Daniels, A. D.; Kudin, K. N.; Strain, M. C.; Farkas, O.; Tomasi, J.; Barone, V.; Cossi, M.; Cammi, R.; Mennucci, B.; Pomelli, C.; Adamo, C.; Clifford, S.; Ochterski, J.; Petersson, G. A.; Ayala, P. Y.; Cui, Q.; Morokuma, K.; Malick, D. K.; Rabuck, A. D.; Raghavachari, K.; Foresman, J. B.; Cioslowski, J.; Ortiz, J. V.; Stefanov, B. B.; Liu, G.; Liashenko, A.; Piskorz, P.; Komaromi, I.; Gomperts, R.; Martin, R. L.; Fox, D. J.; Keith, T.; Al-Laham, M. A.; Peng, C. Y.; Nanayakkara, A.; Gonzalez, C.; Challacombe, M.; Gill, P. M. W.; Johnson, B. G.; Chen, W.; Wong, M. W.; Andres, J. L.; Head-Gordon, M.; Replogle, E. S.; Pople, J. A. *Gaussian 98*, revision A.7; Gaussian, Inc.: Pittsburgh, PA, 1998..

(31) Diaz, N.; Suarez, D.; Merz, K. M., Jr. *J. Am. Chem. Soc.* **2000**, *122*, 4197−208.

(32) Krauss, M.; Gilson, H. S. R.; Gresh, N. *J. Phys. Chem. B* **2001**, *105*, 8040−9.